Design of Cyclic Fixed-Bed Adsorption Processes

Part I: Phenol Adsorption on Polymeric Adsorbents

A model for the adsorption of phenol in a fixed bed of a polymeric adsorbent is developed. Model parameters (equilibrium parameters, capacity factor, axial dispersion, film mass transfer coefficient, and intraparticle effective diffusivity) are experimentally determined from independent experiments. Numerical solution of the model equations uses the method of lines with double orthogonal collocation in finite elements. The model is used for the prediction of breakthrough curves and is part of a package for the design of cyclic processes.

CARLOS COSTA and ALIRIO RODRIGUES

Department of Chemical Engineering
University of Porto
4099 Porto Codex, Portugal

Scope

Most studies of phenol removal by adsorption deal with granular activated carbon(GAC) in fixed-bed operation. A first objective of this work is to investigate the possibility of using macroreticular resins (e.g., Duolite ES861, Duolite Int.) as an alternative to activated carbon. Moreover, most published models are related to the saturation step of the process. However fixed-bed adsorption is a cyclic process involving three main steps: saturation (load), regeneration (desorption), and washing. Regeneration efficiency in particular is a critical factor for the economy of the overall process. The second objective of the work is to develop and test a model for the saturation step using an adequate methodology for the measurement of model parameters. In part II (Costa and Rodrigues, 1985) this model is coupled to a model for the regeneration step in order to build a package for the design of cyclic fixed-bed adsorbers.

CONCLUSIONS AND SIGNIFICANCE

A mathematical model for the adsorption of phenol in a fixed bed of polymeric adsorbent (Duolite ES861) under isothermal operation was developed. The model takes into account the nonlinear adsorption equilibrium isotherm of Langmuir-type hydrodynamics described by an axial dispersion flow, and resistances to mass transfer both in the film and inside the particles (pore diffusion). The model contains six parameters: equilibrium parameters (K_L and Q), capacity factor (ξ), Peclet number (Pe), number of film mass transfer units (N_f), and number of intraparticle mass transfer units (N_D).

The methodology used in this work involves the following steps:

1. Measurement of model parameters from independent experiments in adequate laboratory systems, i.e., batch adsorber for equilibrium runs, shallow bed for film mass transfer studies, tracer methods for axial dispersion determinations, and Carberry-type adsorber for diffusivity measurements.
2. Use of appropriate numerical methods to solve the system of partial differential equations containing two spatial coordinates (axial position in the bed and radial position in the particle) and time. The method of lines with double orthogonal collocation was successfully used to solve the complex model equations.
3. Use of the model to predict the influence of the model parameters and to compare predicted and experimental breakthrough curves.

In order to apply this methodology we first looked at the controlling mechanisms for mass transfer at *the particle level.* The pore diffusion model was found to be an adequate model in our operating conditions. With regard to the saturation efficiency, polymeric adsorbents appear to be competitive with activated carbons. This information was integrated in the fixed-bed model which is now ready to be coupled with the model for the regeneration step.

Correspondence concerning this paper should be addressed to Alirio Rodrigues.

INTRODUCTION

The removal of organic pollutants is often achieved by using adsorption on activated carbon either in fixed beds (Svedberg, 1975; Neretnieks, 1976; Peel et al., 1981; Fritz et al., 1981; Merk et al., 1981) or fluidized bed (Ganho et al., 1975). Most studies deal with the development of a mathematical model for the saturation (load or adsorption) step of the process. More recently, polymeric adsorbents have been available in the market as an alternative to activated carbon for the removal of organics. It has been claimed that regeneration of such adsorbents is easier and recovery of pollutants is often possible. Some work has been done on investigating diffusion mechanisms inside particles, either for gas adsorption (Gonzalez et al., 1977), ion exchange (Patell and Turner, 1980) or adsorption of organics (Van Vliet and and Weber, 1981).

An important class of organics which can be treated with such polymeric adsorbents are the phenolic compounds which appear in some liquid effuents in concentrations ranging from 40 to 6,000 mg/L or more. The operation of a fixed bed for the removal of such compounds using polymeric adsorbents is carried out in three steps: saturation (adsorption or load), regeneration (desorption), and washing. The ensemble of those steps is a cycle. The simulation of such cycle operation needs a mathematical model for each step. Every mathematical model will be constructed on the basis of conservation equations, equilibrium laws at the fluid solid interface, kinetic laws of mass transport and initial and boundary conditions. However the use of a model for predicting the behavior of a fixed bed implies knowledge of the model parameters (equilibrium data, film mass transfer coefficient, intraparticle diffusivity, axial dispersion) which can be measured, predicted by existing correlations, or optimized from laboratory experiments.

In this work we adopted the following methodology: each model parameter is independently measured; that is, experiments are designed to determine given parameter free of the influence of other undetermined model parameters. The experimentally measured parameters are then fed to the global model in order to simulate the dynamics of an adsorption fixed-bed process.

MODEL DEVELOPMENT

The mathematical model of the saturation step of a fixed-bed adsorption process needs some knowledge about:

- Liquid-solid equilibrium isotherm
- Mechanisms of intraparticle diffusion
- Film mass transfer
- Hydrodynamics

This information was obtained by independent experiments with a test system: phenol-water/Duolite ES861. The ES861 compound is a polymeric adsorbent based on a polystyrene matrix crosslinked with divinylbenzene, produced by Diaprosim (Chauny, France). A particle of such macroreticular resin can be viewed as an ensemble of microspheres with pores among them; this model is supported by photographs obtained with an electronic microscope (Patell and Turner, 1979; Costa, 1983). Some physical characteristics are: BET specific area $S_{BET} = 500$ m^2/g, internal particle porosity $\epsilon_p = 0.437$, average pore diameter $d = 75$ Å (7.5 nm), apparent density $\rho_a = 537$ g dry resin/L resin, and wet density = 1,020 g of wet resin/L resin.

Adsorption Equilibrium Isotherms

Solid-liquid equilibrium data relating the phenol concentration in the solid phase q (expressed as mg of adsorbed phenol per liter of resin) and the phenol concentration in the liquid phase c (expressed as mg solute per liter of solution) have been obtained from batch experiments. Costa and Rodrigues (1983) have shown that in the range of phenol fluid phase concentrations from 0 to 200 mg/L equilibrium data can be fitted by a Langmuir-type equation

$$q = K_L Q \rho_a \frac{c}{1 + K_L c} \tag{1}$$

where q (mg/L of resin) and c (mg/L) are concentrations of solute in the solid and fluid phases, respectively and K_L and Q are the equilibrium parameters. At 20°C we obtained $K_L = 4.3 \times 10^{-3}$ L/mg and $Q = 63.6$ mg/g of dry resin.

Mechanisms of Intraparticle Diffusion

The model describing intraparticle diffusion should be chosen according to the structure of the adsorbent. Electronic microscopy shows that a bead is an agglomerate of microspheres with pores among them (Costa, 1983; Kunin et al., 1962). Several models can be considered:

- A pore-diffusion model.
- A "series" model in which diffusion into the pores is followed by diffusion inside the microspheres.
- A "parallel" model in which diffusion through the pores and inside the microspheres are considered in parallel.

Experimental results obtained in a batch and continuous perfectly mixed adsorber (Carberry-type adsorber) were analyzed by these models; we concluded that in the range of concentrations between 0 and 100 mg/L for phenol solutions the pore diffusion model fits our results well (Costa and Rodrigues, 1983). The measured effective diffusivity was found to be $D_{pe} = 7.7 \times 10^{-10}$ m^2/s which should be included in the particle equation:

$$\frac{\partial q}{\partial t} + \epsilon_p \frac{\partial c_p}{\partial t} = D_{pe}\left(\frac{\partial^2 c_p}{\partial R^2} + \frac{2}{R}\frac{\partial c_p}{\partial R}\right) \tag{2}$$

where c_p is the phenol concentration in the pores and R the radial position in the particles.

Film Mass Transfer Coefficient

Since film mass transfer depends on the hydrodynamic conditions, we used a shallow bed of polymeric adsorbent placed in a fixed bed of glass beads. The kinetic law for mass transfer is:

$$\frac{d\bar{c}_{ev}}{dt} = k_f a_p (c - c_p(R_0)) \tag{3}$$

where $\bar{c}_{ev} = \overline{q + \epsilon_p c_p}$ is a concentration averaged over a particle.

The differential bed of adsorbent is 2.17 cm in diameter; particle diameters used in the experiment were in the range of 0.034–0.077 cm, and flowrates between 25 and 124 mL/min. Figure 1 shows the experimental setup and details of the differential column.

A typical experiment using particle diameter $d_p = 0.06$ cm, flowrate $U = 61.1$ mL/min, feed phenol concentration $c_o = 105$ mg/L, shallow bed of 1.39 cm height inserted between a top layer of glass beads with 0.95 cm and a bottom layer of glass beads of 3.68 cm, leads to the experimental results shown in Figure 2 in terms of outlet reduced concentration $x = c/c_o$ as a function of time t.

A film diffusion model represents well the experimenal results for short times corrsponding to the most abrupt part of the curve with a number of mass transfer units $N_f = 2.0 \pm 0.1$, where $N_f = (1 - \epsilon/\epsilon)(a_p k_f \tau_{sb})$. [$\tau_{sb}$ is the space time for the shallow bed.]

The procedure used takes into account the influence on flow conditions of the top and bottom glass bead layers, axial dispersion, and solute accumulation in the fluid phase. Moreover it takes advantage of a special feature of $x(t)$ curves; these curves (Rodrigues

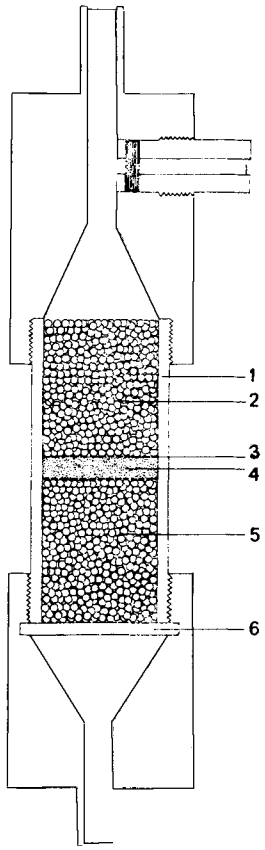

Figure 1a. Experimental setup for shallow bed runs: 1, column; 2&5, glass beads; 3, Inox gauze; 4, shallow bed; 6, porous glass support.

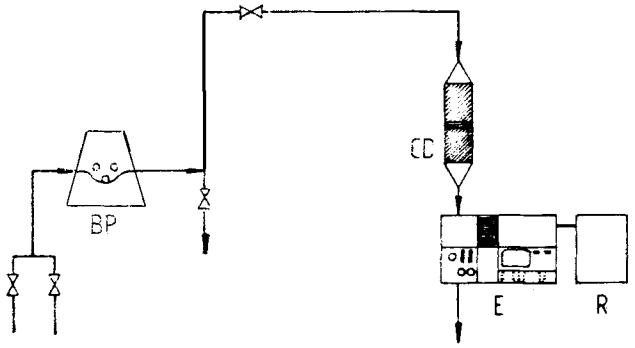

Figure 1b. Experimental setup for shallow bed runs: *BP*, peristhaltic pump; *CD*, shallow bed; *E*, spectrophotometer; *R*, recorder.

et al. 1979) show no influence of internal diffusion for early time (in this case up to $x = 0.3$) for fixed N_f. This was used for optimizing N_f over that region.

The procedure used is more convenient than those based on the Tien and Thodos (1960) method which extrapolates to time zero the value of a global mass transfer coefficient as a function of the adsorbed quantity. By considering that at the initial time only film mass transfer resistance is important, they were able to obtain k_f values.

Experimental results were fitted by a correlation in terms of $j_D = f(Re')$ where the Chilton-Colburn factor $j_D = Sh/Re_o Sc^{1/2}$ and $Re' = Re_o/1 - \epsilon$, with $Re_o = u_o d_p/\nu$, $Sc = \nu/D$, and $Sh = k_f d_p/D$. In the range of our work

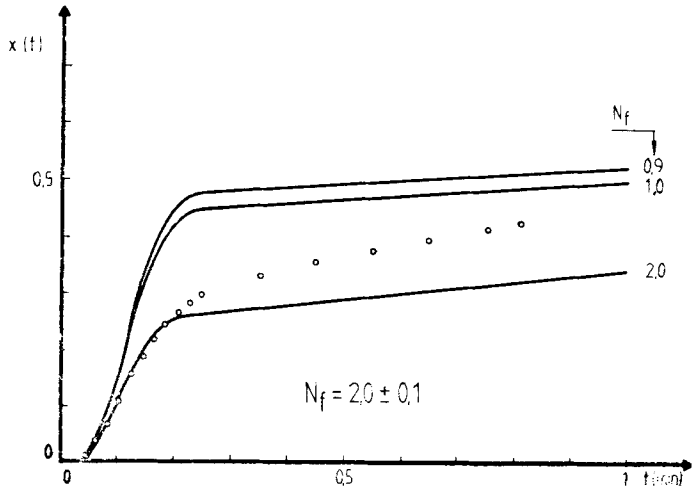

Figure 2. Shallow bed experimental results and model simulations considering only film diffusion N_f, showing optimized value.

$$j_D = 7.32\, Re'^{-0.569} \tag{4}$$

This correlation was later used to calculate N_f values for the simulation of fixed-bed experimental results.

Hydrodynamics

Fluid flow through the adsorption column is well characterized by using the concept of residence time distribution (RTD). Information on RTD was obtained through tracer experiments using a Dirac impulse of tracer (KCl or dye). Results were simply explained by a dispersion model; it should be stated that diffusion of tracer in particle pores was included. The transfer function of the system is:

$$G(s) = \exp\left\{\frac{Pe}{2}\left(1 - \sqrt{1 + \frac{4}{Pe}\left[s + \frac{1-\epsilon}{\epsilon}\epsilon_p \gamma_D(s)\right]}\right)\right\} \tag{5}$$

with

$$\gamma_D(s) = 6N_D \sum_{n=1}^{\infty} \frac{s}{s + N_D n^2 \P^2} \tag{6}$$

where $Pe = u_t L/D_{ax}$ (Peclet number) and $N_D = \tau D_{pe}/R_o^2$ (number of internal mass transfer units).

The model includes four parameters, ϵ, ϵ_p, N_D, and Pe, which were obtained by multivariable optimization (Rosenbrook method); to do that, experimental results are compared with "model" results obtained by inversion of the transfer function using fast Fourier transform technique.

For KCl experiments we used a particle porosity value given by the manufacturer, $\epsilon_p = 0.437$, since the molecule can diffuse into particle pores. However for the dye tracer we did not know the molecule size and the particle porosity available to the tracer was estimated. We found very low values of ϵ_p by optimization, indicating that the dye tracer only slightly diffuses in the adsorbent.

Results are shown in Figure 3, where we plot the particle Peclet number, $Pe_p = u_t d_p/D_{ax}$, as a function of the Reynolds number, $Re = Re_o/\epsilon$.

MATHEMATICAL MODEL

The saturation step of the adsorption process will be considered as isothermal. Moreover the experimental information described before enables us to consider hydrodynamics represented by a

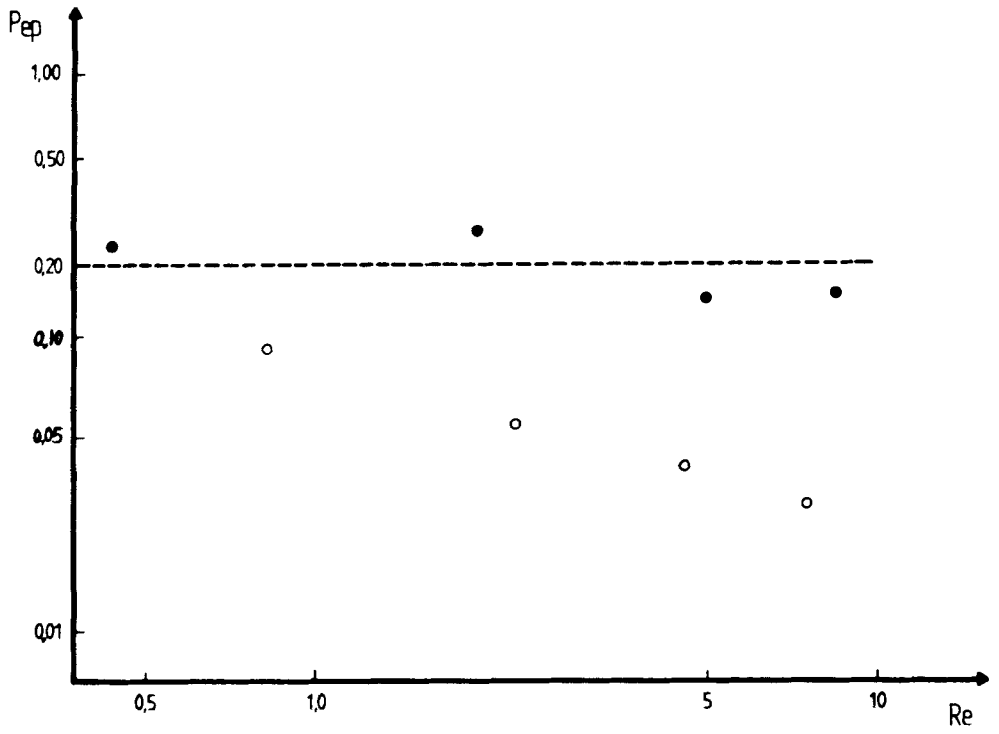

Figure 3. Results obtained in tracer fixed-bed experiments expressed in Pe_p as a function of Reynolds number.

○ KCl tracer; Plexiglass column, 2.18 cm I.D.

● Dye tracer; glass column, 3 cm ID

plug-diffusional model. Intraparticle mass transfer in the macroreticular adsorbent is described by a pore-diffusion model and film mass transfer is taken into account.

The model equations can be written in dimensionless form by introducing a set of variables: $x = c/c_o$ reduced phenol concentration in the fluid phase; $x_p = c_p/c_o$ reduced phenol concentration in the pores; $z^* = z/L$ reduced axial coordinate; $R^* = R/R_o$ reduced radial coordinate for the particle; and $\theta = t/[\tau(1 + \xi)]$ a reduced time [where $\tau = L/u_i$ is the space time and $\xi = (1 - \epsilon)\cdot q_o/\epsilon c_o$ is a capacity parameter]. Taking into account the equilibrium law at the solid-fluid interface, Eq. 1 and the kinetic law for film mass transfer, Eq. 3, we get:

Mass Conservation of Phenol in the Fluid Phase

$$\frac{1}{Pe}\frac{\partial^2 x(z^*,\theta)}{\partial z^{*2}} = \frac{\partial x(z^*,\theta)}{\partial z^*} + \frac{1}{1+\xi}\frac{\partial x(z^*,\theta)}{\partial \theta} + N_f[x(z^*,\theta) - x_p(1,z^*,\theta)] \quad (7)$$

Mass Conservation of Phenol in the Adsorbent Particle

$$\frac{\partial x_p(R^*,z^*,\theta)}{\partial \theta} = \frac{(1+\xi)N_D}{\epsilon_p + \dfrac{K_L Q \rho_a}{(1 + K_L c_o x_p)^2}} \times \left[\frac{2}{R^*}\frac{\partial x_p(R^*,z^*,\theta)}{\partial R^*} + \frac{\partial^2 x_p(R^*,z^*,\theta)}{\partial R^{*2}}\right] \quad (8)$$

Initial and Boundary Conditions for Particle Equation

$$R^* = 0, \frac{\partial x_p(R^*,z^*,\theta)}{\partial R^*} = 0 \text{ (symmetry condition)} \quad (9)$$

$$R^* = 1, 3\xi N_D \frac{\partial x_p(R^*,z^*,\theta)}{\partial R^*} = N_f \frac{K_L Q \rho_a}{1 + K_L c_0}[x(z^*,\theta) - x_p(1,z^*,\theta)] \quad (10)$$

$$\theta = 0, x_p(R^*,z^*,\theta) = 0 \quad (11)$$

Initial and Boundary Conditions for the Fixed-Bed Adsorber

$$z^* = 0, x(z^*,\theta) = 1 \quad (12)$$

$$z^* = 1, \frac{\partial x(z^*,\theta)}{\partial z^*} = 0 \quad (13)$$

$$\theta = 0, x(z^*,\theta) = 0 \quad (14)$$

In the above equations the model parameters are:

- K_L and Q, which characterize the equilibrium adsorption isotherm
- ξ, mass capacity parameter
- Pe, Peclet number; compares the dispersion to the convective flows in the bed
- N_f, number of film mass transfer units; compares the space time with the characteristic time for film diffusion
- $N_D = D_{pe}\tau/R_o^2$, number of intraparticle mass transfer units; compares the space time with the characteristic time for intraparticle diffusion.

One should note that Eq. 10 is obtained by taking the derivative of the solute concentration averaged over a particle, i.e.,

$$\bar{c}_{ev} = \frac{3}{R_0^3}\int_0^{R_0} R^2(q + \epsilon_p c_p)dR \quad (15)$$

and combining it with Eqs. 1, 2, and 3.

NUMERICAL METHODS

To solve the system of partial differential equations (PDE's), Eqs. 7–14, we will use the method of lines, which transforms the actual system of PDE's into a system of ordinary differential equations of initial-value type. Spatial coordinates are first discretized by using orthogonal collocation (Finlayson, 1980).

Let us first consider the radial particle coordinate. We have shown (Rodrigues et al., 1984) that the solution of pore-diffusion model equations in the case of batch adsorption requires collocation on finite elements (Carey and Finlayson, 1975) in order to guarantee stable profiles and to avoid a large number of collocation points (more than 20) if global collocation were used. The discretization involves the use of base functions; we choose Hermite polynomials, which present some advantages compared with Lagrange polynomials for collocation on finite elements in this case. In fact they can be defined in such a way that continuity of the tentative solution and its derivative in each knot (subinterval frontier) is automatically insured; this avoids two additional equations for each knot. However we should point out that some disadvantages also exist; namely that the use of Hermite polynomials leads to systems of differential equations in the implicit form, which implies the need of two matrix inversions.

Let us consider now Eq. 8 together with its initial and boundary conditions, Eqs. 9, 10, and 11. Because of the symmetry of the problem relative to $R^* = 0$ we will make the change of variable $u^* = R^{*2}$.

We consider the domain of the radial coordinate u^* divided into Ne subintervals. The trial solution in the subinterval k can be represented (Finlayson, 1980) by

$$S(g_k,z^*,\theta) = \sum_{I=1}^{4} a_I(z^*,\theta)H_I(g_k) \tag{16}$$

where $H(g)$ are cubic Hermite polynomials defined over the subinterval k,a_I are coefficients to be calculated, and g_k is the normalized radial coordinate for this subinterval, i.e.

$$g_k = \frac{u^* - u_k^*}{h_k} \text{ with } h_k = u_{k+1}^* - u_k^* \tag{17}$$

where u_k^* and u_{k+1}^* are the lower and upper limits for the subinterval k.

The application of the orthogonal collocation method implies knowledge of the $H(g_k)$ as well as its first and second derivatives in the collocation points (represented here by A and B) which are given by Finlayson (1980).

Applying collocation with these base functions to Eq. 8 and its boundary conditions we get:

Boundary Condition for $R^* = 0$

$$\frac{1}{h_1}\sum_{I=1}^{4} A_I a_I = 0 \text{ which gives } a_2 = 0 \tag{18}$$

First Subinterval

$$H_{j1}\frac{\partial a_1}{\partial \theta} + \sum_{I=3}^{4} H_{jI}\frac{\partial a_{I-1}}{\partial \theta} = \frac{(1+\xi)N_D}{\epsilon_p + \dfrac{K_L Q \rho_a}{\left[1 + K_L c_o\left(H_{j1}a_1 + \sum_{I=3}^{4} H_{jI}a_{I-1}\right)\right]^2}} \cdot \left[\frac{6}{h_1}A_{j1}a_1 + \frac{4g_j}{h_1^2}B_{j1}a_1 + \frac{6}{h_1}\sum_{I=3}^{4} A_{jI}a_{I-1} + \frac{4g_j}{h_1^2}\sum_{I=3}^{4} B_{jI}a_{I-1}\right] \quad j = 1,2 \tag{19}$$

2nd to NE-1 Subintervals

$$\sum_{I=1}^{4} H_{jI}\frac{\partial a_{I+2k-3}}{\partial \theta} = \frac{(1+\xi)N_D}{\epsilon_p + \dfrac{K_L Q \rho_a}{\left[1 + K_L c_o \sum_{I=1}^{4} H_{jI}a_{I+2k-3}\right]^2}} \cdot \left[\frac{6}{h_k}\sum_{I=1}^{4} A_{jI}a_{I+2k-3} + \frac{4g_j}{h_k^2}\sum_{I=1}^{4} B_{jI}a_{I+2k-3}\right] \quad \begin{matrix} j = 1,2 \\ k = 2,\ldots,NE-1 \end{matrix} \tag{20}$$

Boundary Condition for $R^* = 1$

$$a_{2NE+1} = \frac{N_f}{6\xi N_D}\frac{K_L Q \rho_a}{1 + K_L c_o}(x(z^*,\theta) - a_{2NE}) \tag{21}$$

this coefficient a_{2NE+1} wil be also taken into account in the equations for subinterval NE.

NE Subinterval

$$\sum_{I=1}^{3} H_{jI}\frac{\partial a_{I+2NE-3}}{\partial \theta} + H_{j4}\frac{\partial a_{2NE+1}}{\partial \theta} = \frac{(1+\xi)N_D}{\epsilon_p + \dfrac{K_L Q \rho_a}{\left[1 + K_L c_o\left(\sum_{I=1}^{3} H_{jI}a_{I+2NE-3} + H_{j4}a_{2NE+1}\right)\right]^2}} \cdot \left[\frac{6}{h_{NE}}\sum_{I=1}^{3} A_{jI}a_{I+2NE-3} + \frac{4g_j}{h_{NE}^2}\sum_{I=1}^{3} B_{jI}a_{I+2NE-3} + \left(\frac{6}{h_{NE}}A_{j4} + \frac{4g_j}{h_{NE}^2}B_{j4}\right)a_{2NE+1}\right] \quad j = 1,2 \tag{22}$$

This leads to a system of $2NE$ implicit PDE's in only one spatial dimension (axial coordinate). With regard to the subintervals a nonuniform grid will be used, concentrating more subintervals near $R^* = 1$ since the radial profiles are sharper in this zone.

Using the methodology described elsewhere (Rodrigues et al., 1984) we concluded that ten subintervals are needed, the knots being located at 0, 0.25, 0.64, 0.685, 0.73, 0.775, 0.82, 0.865, 0.91, 0.955, and 1.

For the initial condition, Eq. 11, and taking into account Eqs. 18 and 21, we get:

1st Subinterval

$$H_{j1}a_1 + \sum_{I=3}^{4} H_{jI}a_{I-1} = 0 \qquad j = 1,2 \tag{23}$$

2nd to $NE - 1$ Subintervals

$$\sum_{I=1}^{4} H_{jI}a_{I+2k-3} = 0 \qquad \begin{matrix} j = 1,2 \\ k = 2,\ldots,NE-1 \end{matrix} \tag{24}$$

TABLE 1. PRECISION AND OSCILLATION NATURE OF PROFILES

	Number of Subintervals			
Pe	10	15	20	30
50	Precision*	—	—	—
	No osc.**			
100	Precision	—	—	—
	−0.001–1.003	No osc.	—	—
150	precision	—	—	—
	−0.014–1.02	−0.0008–1.01	No osc.	—
200	—	Precision	—	—
	−0.014–1.03	−0.006–1.03	0–1.005	No osc.

* Precision reached.
** No oscillations.

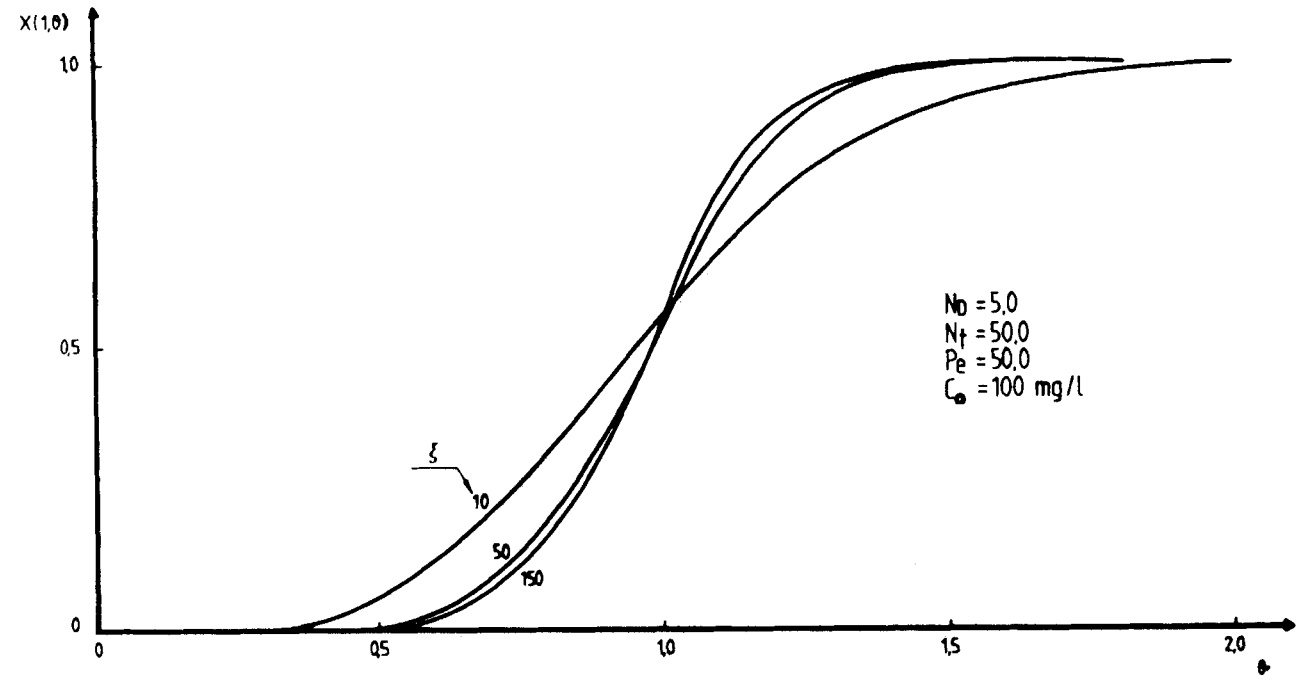

Figure 4. Influence of the capacity parameter ξ on the fixed-bed response to a step input.

NE Subinterval

$$\sum_{I=1}^{2} H_{jI} a_{I+2NE-3} + \left(H_{j3} - H_{j4}\frac{N_f}{6\xi N_D}\frac{K_L Q \rho_a}{1 + K_L c_o}\right) a_{2NE}$$
$$= -H_{j4}\frac{N_f}{6\xi N_D}\frac{K_L Q \rho_a}{1 + K_L c_0} x(z^*,0) \qquad j = 1,2 \quad (25)$$

This system of $2NE$ algebraic equations can be solved in order to get the initial values for the coefficients a which are dependent on the initial solute concentration in the interstitial phase, $x(z^*,0)$.

After discretization of the radial coordinate a system of $2NE + 1$ one-dimensional PDE's is obtained, i.e., Eq. 7 plus $2NE$ equations, Eqs. 19, 20, and 22. The problem is now solved with the PDECOL package (Madsen and Sincovec, 1979) which uses a finite element collocation technique for the discretization of the spatial coordinate,

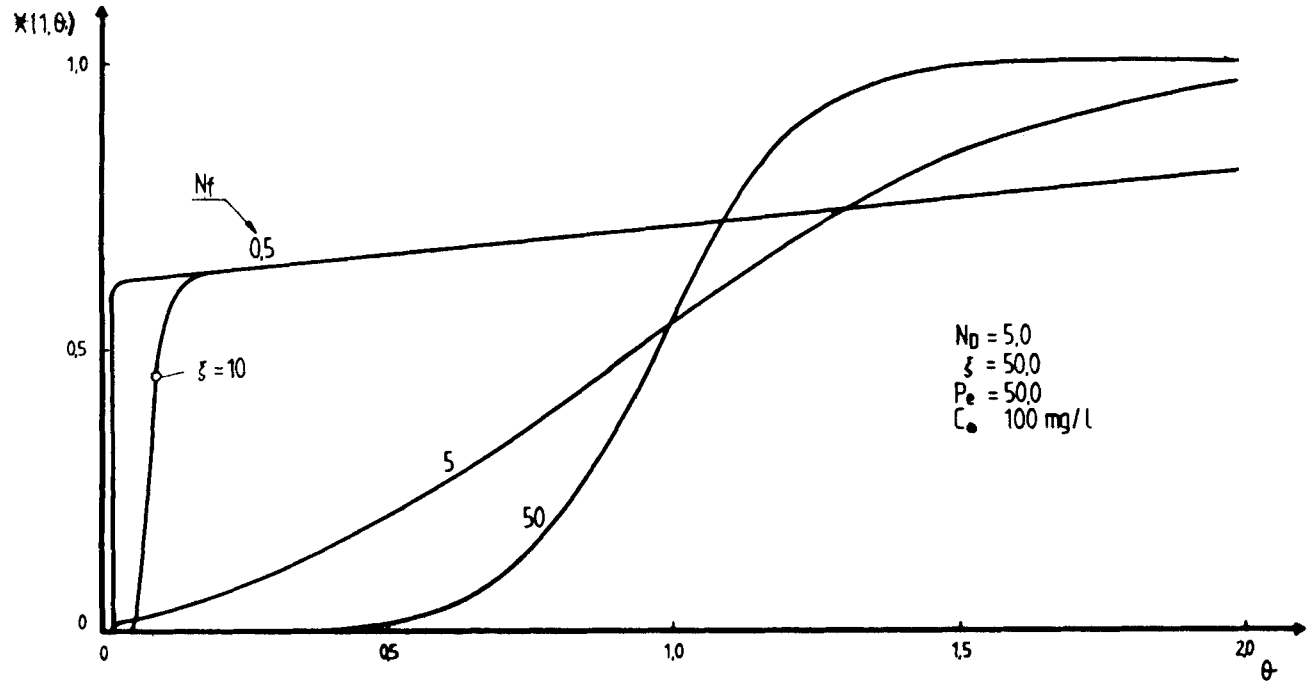

Figure 5. Influence of the number of film mass transfer units N_f on the fixed-bed response to a step input.

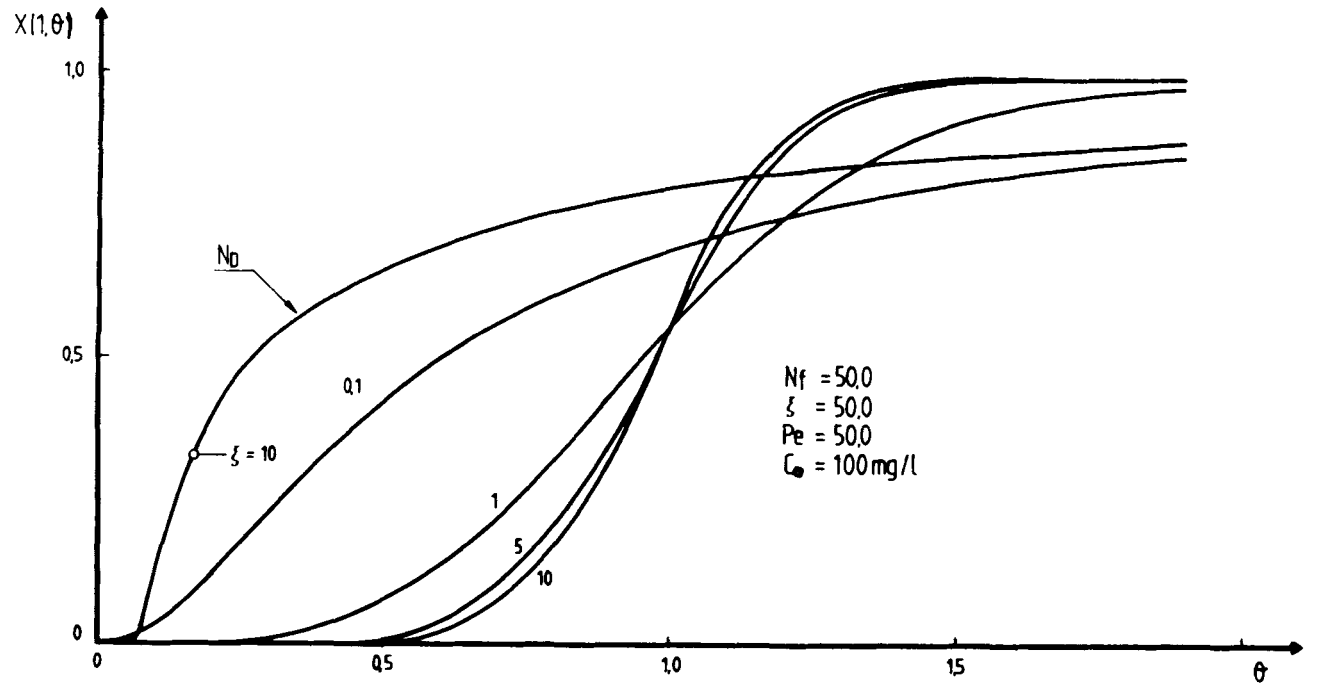

Figure 6. Influence of the number of intraparticle mass transfer units N_D on the fixed-bed response to a step input.

and a modified version of GEARIB (Hindmarsh, 1976) for solving the resulting initial value problem.

The adsorption equilibrium theory predicts sharp profiles in fixed beds when the equilibrium isotherm is favorable. On the other hand diffusional phenomena count as dispersive factors, leading to a broadening of the profile, i.e., the conservation equation for the fluid phase becomes more parabolic.

The polynomial representation of these profiles generally implies the use of many subintervals (the profile is relatively sharp and is moving in the bed) which in the case of high Peclet number ($Pe > 500$) lead to high dimensionality problems; the solution by fixed grid finite elements is then not convenient. For these cases (quasihyperbolic equations) a methodology has been recently developed using moving finite elements (Gelinas et al., 1981). In the

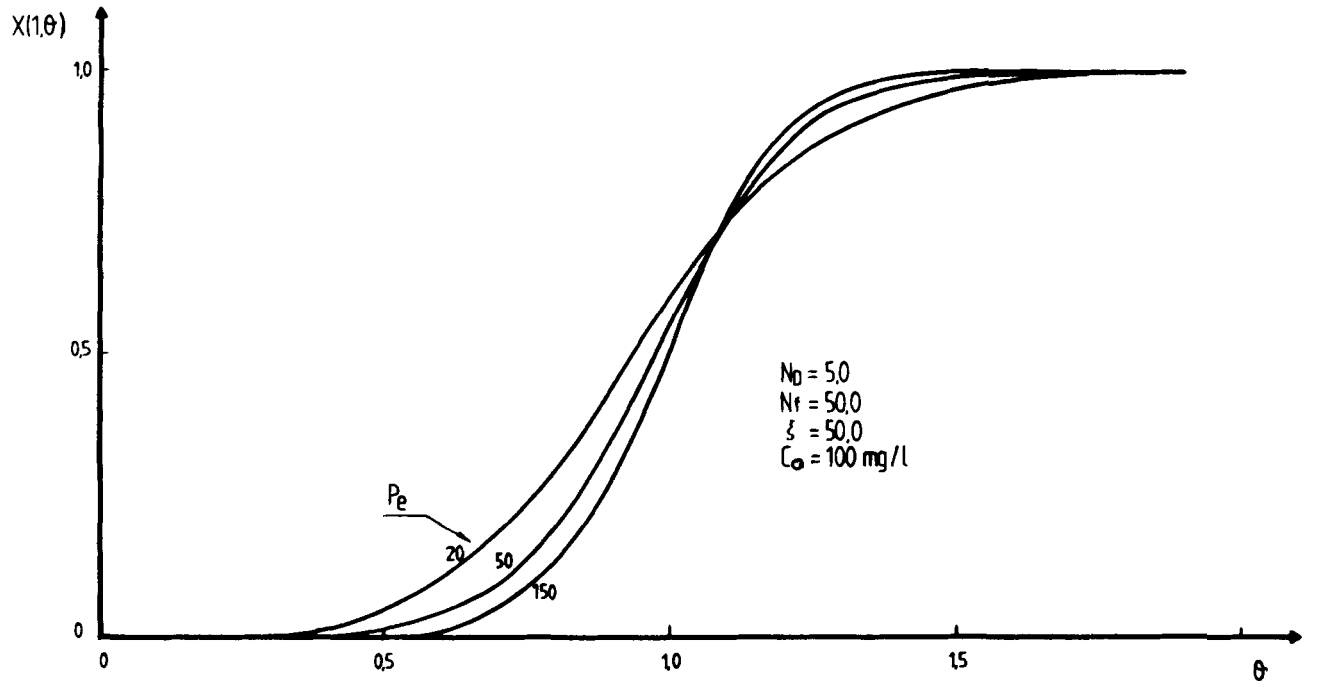

Figure 7. Influence of the Peclet number *Pe* on the fixed-bed response to a step input.

TABLE 2. EXPERIMENTAL CONDITIONS FOR FIXED-BED RUNS (PHENOL ADSORPTION IN Duolite ES861)

Run	U mL/min	c_o mg/L	t_{st} min	ξ	$\tilde{Q}_T$ mg
1	158.7	82.0	47.6	93.6	619.7
2	115.2	91.6	62.2	79.7	655.8
3	54.4	91.6	134.6	82.7	670.2
4	16.8	82.4	455.5	95.1	630.7

TABLE 3. MODEL PARAMETERS DETERMINED BY INDEPENDENT EXPERIMENTS

Run	ξ	N_f	N_D	Pe
1	93.6	36.3	0.261	18.7
2	71.7	35.8	0.395	24.0
3	82.7	57.0	0.824	36.0
4	95.1	132.6	2.468	68.0

present work we limited our simulations to Peclet numbers lower than 200 in order to make possible the use of finite elements with a fixed grid for the numerical solution of the problem.

In order to use the PDECOL package some preliminary tests are needed with the objective of choosing the number and localization of the subintervals when cubic interpolation functions are used.

The tests were performed with a model similar to that described here but with no film mass transfer and no intraparticle resistance. This model will give a profile sharper than the corresponding to the model developed above. Then we are testing a less favorable case and the conclusions will be quite conservative.

Several simulations were carried out using various Peclet numbers (50, 100, 150, and 200) and different numbers of subintervals (10, 15, 20, and 30).

Two characteristics were analyzed from these results: (i) precision was reached when the history of concentration for a certain number of intervals was equal (10^{-3}) with the history obtained for a higher number of subintervals; and (ii) we considered the higher absolute values of dependent variables above 1 and below 0.

Table 1 shows the results of this simulation study. According to these results, and considering that our profiles are more dispersive than the ones being treated, we will use ten subintervals for $Pe <= 150$ and 15 subintervals for $150 < Pe <= 200$.

SIMULATION RESULTS

The mathematical model for the saturation step of the fixed-bed adsorption process is a system of parabolic PDE's with two spatial dimensions: axial and radial coordinates.

The computer simulation using the numerical method described above enables us to study the influence of the model parameters. In the simulations the equilibrium parameters, i.e., K_L and Q, as well as the feed concentration c_o were kept constant.

Influence of the Mass Capacity Parameter, ξ

The effect of ξ over the breakthrough curves is shown in Figure 4. Efficiency of solute removal increases when ξ increases, since breakthrough curves are then less-dispersed around $\theta = 1$.

Influence of the Number of Film Mass Transfer Units, N_f

In Figure 5 the influence of N_f is shown. Higher film mass transfer coefficients or higher N_f leads to better saturation efficiency. However when film mass transfer is important (low N_f), there is a plateau in the breakthrough curve. In this case, film mass transfer is the controlling step and the effect of ξ on the efficiency of adsorption is reversed relative to the statement made in the previous paragraph (see cures for $N_f = 0.5$ and $\xi = 10$ and 50 in Figure 5). This behavior had already been noticed by Rodrigues and Beira (1979) for a perfectly mixed adsorber.

Influence of the Number of Intraparticle Mass Transfer Units, N_D

In Figure 6 the effect of pore diffusion is shown. When N_D increases, i.e., the resistance to pore diffusion decreases, the efficiency of saturation is better and the breakthrough curves become almost symmetric relatively to $\theta = 1$. In the range of low N_D values the effect of ξ is also reversed although to a smaller extent than in the case of film mass transfer control.

Influence of Axial Dispersion, Pe

Figure 7 shows that with increasing Peclet number, i.e., decreasing axial dispersion effects, the breakthrough curves tend to the solution of the plug flow case. However for high Peclet numbers the effect over the breakthrough curve is not important provided that other dispersive effects are present (e.g., pore diffusion).

EXPERIMENTAL

In order to test the validity of our mathematical model with all the model parameters already determined by independent experiments, we carried out several runs in fixed-bed adsorption columns.

The experimental set-up is similar to that shown in Figure 1b. A Plexiglass column of 2.18 cm I.D. and 40 cm length was used instead of the shallow bed (*CD*). Phenol concentration in the effluent was measured with a UV-spectrophotometer at 272 nm and flow was insured by a peristaltic pump.

In all experiments the initial condition of the bed is zero concentration of phenol (clean bed) and a step change in feed concentration is made. The stoichiometric time defined as $t_{st} = \tau(1 + \xi)$ is directly calculated from experimental breakthrough curves by

$$t_{st} = t_f - \frac{1}{c_o}\int_0^{t_f} c(t)dt \tag{26}$$

where t_f is the time at which $c(t) = c_o$.

Bed porosity is also calculated by

$$\epsilon = \frac{Uc_o t_{st} - Vq_o}{Vc_o - Vq_o} \tag{27}$$

where q_o is the phenol concentration in the saturated particles, i.e.,

$$q_o = \epsilon_p c_o + \frac{K_L Q \rho_a c_o}{1 + K_L c_o} \tag{28}$$

where V is the fixed bed volume.

From these results we can also get:

$$\text{Mass capacity factor} \qquad \xi = \frac{t_{st}U}{\epsilon V} - 1 \tag{29}$$

$$\text{Total capacity of the fixed bed } \tilde{Q}_T = t_{st}Uc_o \tag{30}$$

Table 2 shows the experimental conditions used in various runs where the flowrate was changed.

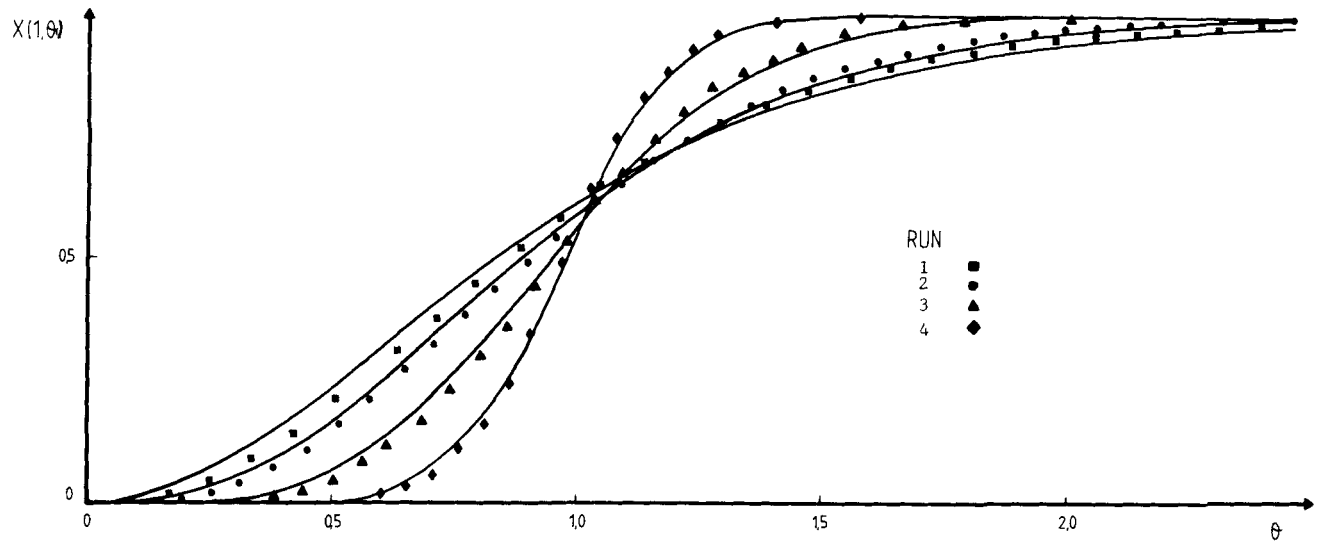

Figure 8. Experimental and simulated concentration histories for fixed-bed runs.

Simulation of Fixed-Bed Experiments

For simulation purposes we used model parameters already determined; the values are given in Table 3. Figure 8 shows the experimental and simulated results for the experimental conditions listed in Table 2.

The model predictions are in reasonable agreement with the experimental results. The methodology seems to be interesting since the model parameters retain a physical meaning and can be determined from relatively simple experiments.

CONCLUSIONS

The methodology followed for studying isothermal single component adsorption in fixed beds consists of several steps:

1. Measuring the parameters governing the dynamic behavior of fixed-bed adsorbers from independent experiments.
2. Developing a mathematical model and appropriate numerical methods for the solution of model equations.
3. Using the model for prediction of breakthrough curves and incorporating it in a package for the design of cyclic fixed-bed processes.

The model can also be used for simulation studies in order to develop shortcut methods for the design of fixed-bed adsorbers. As an example, graphs plotting the breakthrough time as a function of model parameters can easily be constructed. The main advantage of such a procedure is that model parameters are physically meaningful, and it can be extended to multicomponent systems.

The analysis of the governing intraparticle diffusion mechanisms is based on experiments carried out in batch or continuous perfectly mixed adsorbers. Once we know which intraparticle diffusion mechanism is important, the fixed-bed model is developed. Numerical solution of the resulting system of PDE's is not straightforward, particularly when sharp profiles (concentration wave) travel through the fixed bed. Moreover, filling up an adsorbent particle is in the first stages a quite complex numerical problem due to the sharp radial profile which develops. Then a careful simulation of these radial profiles was carried out before setting the conditions for a successful use of algorithm.

The predicted breakthrough breakthrough curves agree well with the experimental curves. It should be stressed that the model parameters are not fitted from the experimental breakthrough curves; they were determined from independent experiments in various types of adsorption equipment.

The model for the saturation (or load) of a fixed bed should now be combined with a model for the regeneration of polymeric adsorbents saturated with phenol in order to develop a computer package for the design of cyclic fixed bed adsorption processes. This is done in Part II.

ACKNOWLEDGMENT

We are grateful to JNICT, INIC, and the Gulbenkian Foundation for financial support.

NOTATION

A	= first derivatives matrix (Hermite polynomials)
$a_I(z^*,\theta)$	= coefficients of the trial solution
a_p	= specific area, L^{-1}
B	= second derivatives matrix (Hermite polynomials)
c	= fluid phase concentration, ML^{-3}
$\bar{c}_{ev}$	= average solute concentration in the particles, ML^{-3}
c_p	= solute concentration in the pores, ML^{-3}
c_o	= input concentration, ML^{-3}
D	= molecular diffusivity at infinite dilution, L^2T^{-1}
D_{ax}	= axial dispersion, L^2T^{-1}
D_{pe}	= effective pore diffusivity, L^2T^{-1}
d_p	= particle diameter, L
g_k	= subinterval normalized radial coordinate
$H_I(g_k)$	= Hermite polynomials over the subinterval k
h_k	= length of subinterval k
j_D	= Chilton-Colburn factor
K_L	= isotherm parameter, L^3M^{-1}
k_f	= film mass transfer coefficient, LT^{-1}
L	= fixed bed length, L
NE	= number of subintervals
N_D	= number of intraparticle mass transfer units $=D_{pe}\tau/R_o^2$
N_f	= number of film mass transfer units $= (1-\epsilon)/\epsilon\, a_p k_f \tau$
Pe	= Peclet number
Pe_p	= particle Peclet number

Q = isotherm parameter, MM^{-1} (dry resin)
Q_T = fixed bed total capacity, M
q = concentration in the solid phase; ML^{-3}
q_o = solid phase concentration in equilibrium with c_o, ML^{-3}
R = radial coordinate, L
R^* = normalized radial coordinate in particle
R_o = particle radius, L
Re = Reynolds number
Re' = modified Reynolds number
Re_o = modified Reynolds number
Sc = Schmidt number
Sh = Sherwood number
s = Laplace variable
t = time, T
t_f = time at which output concentration reaches input concentration
t_{st} = stoichiometric time, T
U = flow rate, L^3T^{-1}
u^* = normalized radial coordinate
u_k^* = inferior limit of subinterval k
u_i = interstitial velocity, LT^{-1}
u_o = superficial velocity, LT^{-1}
V = volume of the fixed bed, L^3
x = normalized fluid phase concentration
x_p = normalized concentration in the pores
z = axial coordinate, L
z^* = normalized axial coordinate

Greek Letters

ξ = capacity parameters, $(1 - \epsilon/\epsilon)(q_o/c_o)$
ϵ = porosity
ϵ_p = internal porosity
$\gamma_D(s)$ = defined in Eq. 6
ν = kinematic viscosity, L^2T^{-1}
ρ_a = apparent density, M(dry resin)L^{-3}
θ = normalized time $= t/\tau(1 + \xi)$
τ = space time $= L/u_i$, T
τ_{sb} = shallow bed space time, T

LITERATURE CITED

Carey, G. F., and B. A. Finlayson, "Orthogonal Collocation on Finite Elements," *Chem. Eng. Sci.*, **30**, 587 (1975).

Costa, C., "Dynamics of Cyclic Processes: Adsorption and Parametric Pumping," Ph. D. Thesis, University of Porto, Portugal (1983).

Costa, C., and A. Rodrigues, "Dynamics of Phenol Adsorption on Polymeric Supports," *Fundamentals of Adsorption*, A. Myers, ed., Engineering Foundation (AIChE), New York (1984).

———, "Design of Cyclic Fixed-Bed Adsorption Processes. II: Regeneration and Cyclic Operation," *AIChE J.* (1985).

Finlayson, B. A., *Nonlinear Analysis in Chemical Engineering*," McGraw-Hill, New York (1980).

Fritz, W., and E. Schlunder, "Competitive Adsorption of Two Dissolved Organics onto Activated Carbon. I," *Chem. Eng. Sci.*, **36**, 721 (1981).

Fritz, W., W. Merk, and E. Schlunder, "Competitive Adsorption of Two Organics onto Activated Carbon. II," *ibid*, 731 (1981).

Ganho, R., H. Gilbert, and H. Angelino, "Kinetics of Phenol Adsorption in a Fluidized Bed of Activated Carbon," *Chem. Eng. Sci.*, **30**, 1,231 (1975).

Gelinas, R. J., S. Doss, and K. Miller, "The Moving Finite Element Method: Applications to General Partial Differential Equatioins with Multiple Large Gradients," *J. Comp. Phys.*, **40**, 202 (1981).

Gonzalez, M. G., A. A. Yeramin, and R. E. Cunningham, "Study on the Elucidation of Diffusion Mechanisms in Macroporous Resins," *Rev. Latinoam. Ing. Quim. & Quim. Apl.*, **7**, 39 (1977).

Hindmarsh, A. C., "Preliminary Documentation of GEARIB. Solution of Implicit Systems of Ordinary Differential Equations with Banded Jacobian," Report UCID-30130, Lawrence Livermore Lab., Livermore, CA (1976).

Kunin, R., N. W. Frisch, and S. A. Fisher, "Characteristics of Macrorecticular Ion-Exchange Resins," *Ind. Eng. Chem. Prod. Res. Dev.*, **1**, 140 (1962).

Madsen, N. K., and R. F. Sincovec, "PDECOL-General Collocation Software for Partial Differential Equations," *ACM Trans. Math. Software*, **5**(3), 326 (1979).

Merk, W., W. Fritz, and E. Schlunder, "Competitive Adsorption of Two Organics onto Activated Carbon. III," *Chem. Eng. Sci.*, **36**, 743 (1981).

Neretnieks, I., "Analysis of Some Adsorption Experiments with Activated Carbon," *Chem. Eng. Sci.*, **31**, 1,029 (1976).

Patell, S. and J. R. Turner, "The Equilibrium and Sorption Properties of Some Porous Ion-Exchangers," *J. Sep. Proc. Technol.*, **1**(1), 42 (1979).

———, "The Kinetics of Ion-Exchange Using Porous Exchangers," *J. Sep. Proc. Technol.*, **1**(2), 31 (1980).

Peel, R. G., A. Benedek, and C. M. Crowe, "A Branched Pore Kinetic Model for Activated Carbon Adsorption," *AIChE J.*, **27**(1), 26 (1981).

Rodrigues, A., et al., "Computational Aspects of the Dynamics of Sorption Operations," CACE'79, Montreux (1979).

Rodrigues, A., and E. Beira, "Staged Approached to Percolation Processes," *AIChE J.*, **25**(3), 416 (1979).

Rodrigues, A., et al., "Dynamics of Adsorption Processes," *Stiff Computation*, R. Aiken, Ed., Oxford Univ. Press (1984).

Svedberg, G., "Simulation of Sorption Processes," Ph.D. Thesis, Royal Institute of Technology, Stockholm (1975).

Tien, C., and G. Thodos, "Ion-Exchange Kinetics: The Removal of Oxalic Acid from Glycol Solutions," *Chem. Eng. Sci.*, **13**, 120 (1960).

Van Vliet, B. M., and W. J. Weber, Jr., "Comparative Performance of Synthetic Adsorbents and Activated Carbon for Specific Compound Removal from Wastewaters," *J. WPCF*, 1,585 (Nov. 1981).

Manuscript received Feb. 29, 1984; revision received Oct. 26 and accepted Oct. 29, 1984.